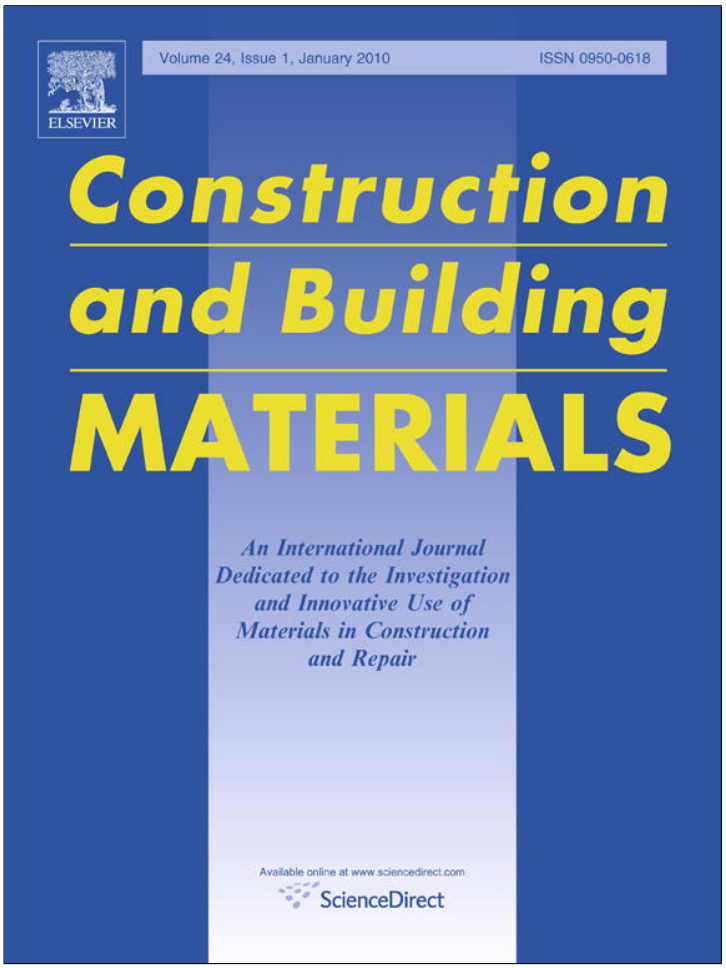

Construction and Building Materials 24 (2010) 1–10

Contents lists available at ScienceDirect

Construction and Building Materials

journal homepage: www.elsevier.com/locate/conbuildmat

Properties of poly(vinyl alcohol) fiber reinforced high-performance organic aggregate cementitious material: Converting brittle to plastic

H. Toutanji [a,*], B. Xu [a], J. Gilbert [b], T. Lavin [c]

[a] Department of Civil and Environmental Engineering, University of Alabama in Huntsville, Huntsville, AL, USA
[b] Department of Mechanical and Aerospace Engineering, University of Alabama in Huntsville, Huntsville, AL, USA
[c] Soems Corporation, Watchung, NJ, USA

ARTICLE INFO

Article history:
Received 10 May 2009
Received in revised form 27 July 2009
Accepted 5 August 2009
Available online 17 September 2009

Keywords:
High-performance
Lightweight
PVB
PVA(polyvinylalcohol) fiber
ITZ, interfacial transition zone
Density
Fracture toughness

ABSTRACT

This study focuses on the development of a lightweight high-performance cementitious composite material which is reinforced with poly(vinyl alcohol) (PVA) fiber and contains poly(vinyl butyral) (PVB) as the sole aggregate. Mechanical properties such as compressive and flexural strengths, impact resistance, and fracture toughness are evaluated. PVB composite produces low average density concrete of 1548 kg/m^3 (96.6 pcf) and a compressive strength of about 40 MPa (5800 psi). The addition of PVA fiber improves ductility, fracture toughness and impact resistance with fiber volume fractions. In general, the increase in fracture toughness is found to be linear with increasing fiber volume fraction, whereas the increase associated with the impact resistance is non-linear. A model based on fiber bridging mechanics and the rule of mixtures is developed to characterize fracture toughness. Comparisons are made with a lightweight concrete having equal density, and a normal-weight concrete. A good correlation is obtained for the materials tested when experimental results are compared to those predicted by the developed model.

1. Introduction

Prior research has shown that by employing poly(vinyl butyral) (PVB) powder as a total replacement for aggregate and using PVA fiber as reinforcement, cementitious composite materials display strong interactions at the molecular level; resulting in improved ductility, impact resistance, fracture toughness and impact resistance, with increasing fiber volume fraction [1,2]. Previous study shows that the interfacial transition zone (ITZ), which is characterized by the prevalence of calcium hydroxide and a higher porosity, is the weakest region that controls many important properties of concrete such as strength, permeability, and durability [3]. During curing of concrete, an area between the bulk cement paste and the aggregate forms which is more porous, less mineralized, and has fewer packed cement particles [4]. The space around the aggregates is less effectively filled by hydration products, and at the same time there is greater tendency for CH ($Ca(OH)_2$) and ettringite to develop in this space. This unfilled space or wall effect in the ITZ has been confirmed by many researchers characterising the microstructure of the ITZ and the hydration progress in the ITZ [5–12]. Methods have been studied to improve the aggregate/matrix bonding in ITZ, such as reducing the size of the aggregates [13,14], using basalt and quartzite as aggregates [15], or replacing the cement by certain amount of ultrafine additions such as silica fume and metakaolin [16–18]. However, these methods are limited since they do not significantly increase the interactions between the atoms and molecules and for the most part involve siliceous aggregates. We chose to use a non-siliceous organic aggregate with a different chemistry than standard aggregates and asked if we saw different types of mechanical effects which could be interpreted as alterations in the ITZ such as toughness. In addition to the aggregate/matrix interface, fiber/matrix debonding by shear type of deformation and fiber sliding wear are the dominant failure mechanisms [19]. Although, steel and glass have high tensile strength, both of them have lower bond strength with concrete and mortars due to the poor bonding at the interface. It is of interest therefore to produce a cement based composite in which the aggregate, the fiber and the matrix could all interact chemically.

Both PVB and PVA contain chemical features which may affect the bonding properties between paste and aggregate. For example, hydroxyl groups which have the potential to form hydrogen bonds between molecules, or within different parts of a single molecule. This special feature could provide remarkable changes in the surface bond strength, not only between the aggregate and the matrix, but also between the fiber reinforcement and the matrix and aggregates. Additionally the ether oxygen functional group acts as a weak base and can interact with lewis acids and electropositive materials such as CSH or magnesium.

* Corresponding author. Fax: +1 2568246724.
E-mail address: toutanji@cee.uah.edu (H. Toutanji).

0950-0618/$ - see front matter © 2009 Elsevier Ltd. All rights reserved.
doi:10.1016/j.conbuildmat.2009.08.023

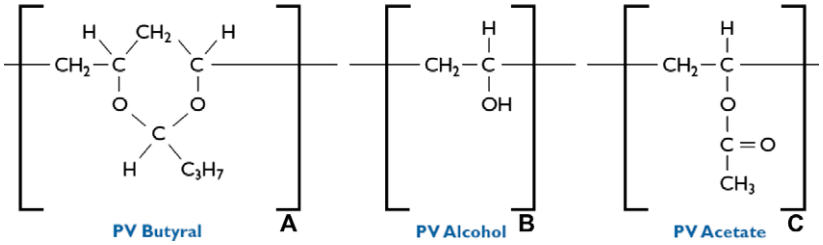

Fig. 1. Structure of poly(vinyl butyral) (PVB) [20].

Poly(vinyl butyral) (PVB) is a high polymer member of the class of poly(vinyl acetal) resins [20]. It is derived by condensing poly(vinyl alcohol) (PVA) with butyraldehyde in the presence of a strong acid. PVA reacts with the aldehyde to form six-membered rings primarily between adjacent intramolecular hydroxyl groups, leading to the structure shown in Fig. 1. The appearance of PVB is a white or light yellow solid free flowing amorphous powder which can totally pass sieves with hole sizes of 0.9 mm. It has a Rockwell hardness (D785-51) between 90 and 100 (M), a tensile strength of approximately 6000 psi and modulus of elasticity of 30,000 psi. The PVB aggregate is completely insoluble in cement water mixes and is highly alkali resistant. PVB is commercially prepared by a well-known reaction between aldehydes and alcohols. The resulting polymer is a terpolymer containing varying amounts of butryal polyvinyl alcohol (PVA), and polyvinyl acetate because of incomplete conversion.

We speculate that our observed mechanical properties may originate from the chemical properties of PVB. The presence of hydroxyl groups in the polymer molecule enables good wetting of most substrates and provides a mechanism to make non-covalent ionic and hydrogen bonds. For example, the hydroxyl groups in PVB polymer provide electrostatic attractive and hydrogen bonding interactions with other substances. This chemical mechanism (process) is illustrated in Fig. 2 using a glass substrate as an example. Cho et al. [21,22] showed that hydroxyl groups of PVB, which originates from the vinyl alcohol units, strongly reacts with boron oxide, which is a major ($\geqslant$50%) component of the borosilicate glass used in his study. And the presence of acetate and relatively non-polar rings provide a mixed hydrophilic hydrophobic character which can affect adhesion and elongation. Additional effects on the cement matrix itself may occur through available ether group interactions which may alter the cement matrix structure or nucleation reaction. We speculate that the functional chemical groups of PVB allow non-covalent bonding to elements of the cement matrix and provide for increased toughness at the PVB aggregate–CSH interface.

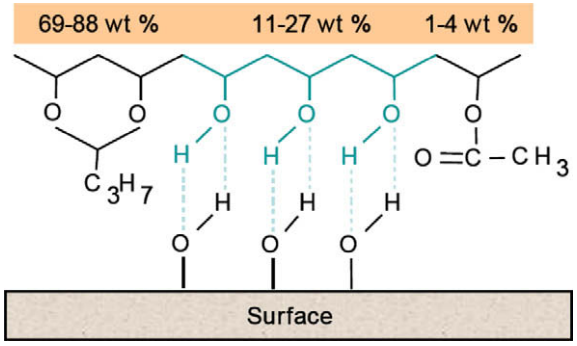

Fig. 2. Adhesion to substrates by hydrogen bond.

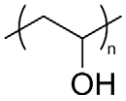

Fig. 3. Structure of poly(vinyl alcohol) (PVA).

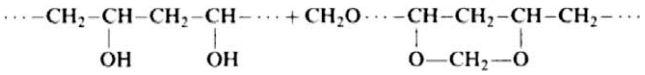

Fig. 4. Formal groups of PVA fiber [24].

Poly(vinyl alcohol) (PVA) is obtained from poly(vinyl acetate) which is readily hydrolyzed by treating an alcoholic solution with aqueous acid or alkali [23], leading to the structure as shown in Fig. 3. PVA is a white powder with a specific gravity in the range of 1.2–1.3 and a glass transition temperature of around 80 °C [24]. This powder may be formed and extruded to become PVA fibers which are commercially produced and sold as concrete additives to produce ECC materials as described by Wang and Li [25]. These fibers are insoluble in water yet are quite hydrophillic. This research is aimed at developing a novel cementitious composite material by utilizing PVB as fine aggregate and PVA fibers as reinforcement to test the hypothesis that using an aggregate with a different chemistry than siliceous aggregate will influence mortar characteristics. Specifically, this research is focused on: (i) developing a lightweight high-performance cementitious material using poly(vinyl butyral) (PVB) reinforced with PVA fiber; (ii) investigating the mechanical properties of PVB concrete such as compressive strength, flexural strength, fracture toughness and impact resistance; (iii) developing a lightweight concrete and a normal-weight concrete to make comparisons; and (iv) developing a model to predict the behavior of fracture toughness (see Fig. 4).

2. Theoretical background

2.1. Ultimate tensile strength by fibers

Li [26] showed that the ultimate tensile strength of a fiber reinforced composite is a function of the fiber, the interface between the fiber and the matrix, and the matrix characteristics. The following equation is derived based on a micromechanical model involving the bridging mechanism of randomly oriented short straight fibers [26]:

$$\sigma_t = \frac{1}{2} V_f g \tau \left(\frac{L_f}{d_f}\right) \tag{1}$$

where V_f, L_f, and d_f are the fiber volume fraction, length of fiber, and the diameter of the fiber, respectively. τ is the fiber/matrix frictional bond strength; and g is a set of interface parameters developed for different fiber types as follows [27]:

$$g = \frac{2}{(4+f^2)}\left(1+e^{f\pi/2}\right) \quad (2)$$

In Eq. (2), f is a snubbing coefficient that must be determined experimentally for a given fiber/matrix system.

The fiber volume fraction can be calculated from the following equation:

$$V_f = \frac{\rho_m W_f}{\rho_f W_m + \rho_m W_f} \quad (3)$$

where W_f is the weight of fibers; W_m is the weight of the matrix; ρ_f is the density of the fibers; and ρ_m is the density of the matrix.

Optimization of the interfacial bond strength can only be achieved when the fiber has a length large enough to provide resistance to fiber pull-out and a sufficiently high fiber modulus of rupture to avoid fiber fracture [28]. If the fiber length used in the mix design is less than a critical length, fiber pull-out will occur. If the fiber length is longer than the critical fiber length, then fiber rupture will be the primary mode of failure.

2.2. Rule of mixtures

At low strains, where the fibers and the matrix behave elastically, the composite modulus, E, is determined by a modulus balance which weights the fiber modulus, E_f, and matrix modulus, E_m, by their corresponding volume fractions V_f and V_m, respectively. Mathematically,

$$E = E_f V_f + E_m V_m \quad (4)$$

Eq. (4) is the well-known rule of mixtures (ROM) for the tensile modulus of a composite material and is applicable when the reinforcing fibers are both continuous and well aligned with stress applied along the direction of the fibers [29]. Eq. (4) may be reformulated to reflect the fact that the matrix and fiber develop the same strain, ε, as follows:

$$\sigma = \sigma_f V_f + \sigma_m V_m \quad (5)$$

Keeping in mind that:

$$V_m = 1 - V_f \quad (6)$$

Eq. (5) becomes:

$$\sigma = \sigma_f V_f + \sigma_m (1 - V_f) \quad (7)$$

Table 1
Mechanical properties of PVA fibers [23].

Tensile strength (MPa)	Elastic modulus (MPa)	Gravity
1.23×10^3	2.95×10^4	1.3

2.3. Matrix fracture toughness

The matrix fracture toughness of plain concrete can be calculated using ASTM E 399 [30], standard test method for linear-elastic plane-strain fracture toughness K_{Ic} of metallic materials, as follows:

$$K_{Ic} = \frac{P}{BW^{0.5}} f\left(\frac{a}{W}\right) \quad (8)$$

where, P is the maximum load applied to a single edge notch bending (SENB) specimen; S is the distance between the supports; B is the specimen width; W is the specimen thickness; a is the notch length; and $f(a/W)$ is a shape function calculated as follows [31]:

$$F\left(\frac{a}{W}\right) = \frac{3\frac{S}{W}\sqrt{\frac{a}{W}}}{2\left(1+2\frac{a}{W}\right)\left(1-\frac{a}{W}\right)^{1.5}}\left\{1.99 - \frac{a}{W}\left(1-\frac{a}{W}\right) \times \left[2.15 - 3.93\left(\frac{a}{W}\right) + 2.7\left(\frac{a}{W}\right)^2\right]\right\} \quad (9)$$

The shape function is developed based on a finite element analysis; solutions of this type are typically fit to a polynomial expression (see Table 1).

3. Sample preparation and testing methods

3.1. Mix proportions

The water to cementitious material ratio of all groups are kept at constant of 0.4. The fiber volume fraction V_f are varied from 0% to 0.9% in each group. For the normal-weight concrete, the cement to sand ratio is 1:3. For the lightweight concrete, the density is about 1500 kg/m^3 (93.6 pcf), which is almost the same as the PVB composite mix. The mix proportion is listed in Table 2. The ce-

Table 3
Special properties of PVB products [20].

Property	Units	Condition	Value
PVOH* content	%	B-79	11.5–13.5
		M-B75H	11–27
Specific gravity	–	B-79	1.083
		M-B75H	1.1
Tensile yield strength	MPa	B-79	40–47
		M-B75H	
Elastic modulus	MPa $\times 10^3$	B-79	1.93–2.0
		M-B75H	
Impact strength	J m^{-1}	Izod, notched, 1.25 × 1.25 cm, B-79	42.7-
		M-B75H	
Glass transition temperature	°C	B-79	62–72
		M-B75H	73

* PVOH is the polyvinyl alcohol (PVA) residual in the PVB polymer.

Table 2
Proportion of the mix (kg/m^3).

	Mix number	Cement	MK	Beach sand	Lightweight sand	B-79	M-B75H	Water	SIKA	PVA fiber	w/c	V_f (%)
Normal-weight concrete	N1	558		1674				223			0.4	0
	N2	558		1674				223		4.1	0.4	0.3
	N3	558		1674				223		8.2	0.4	0.6
	N4	558		1674				223		12.3	0.4	0.9
Lightweight concrete	L1	437		147	728			175			0.4	0
	L2	437		147	728			175		3.9	0.4	0.3
	L3	437		147	728			175		7.8	0.4	0.6
	L4	437		147	728			175		11.7	0.4	0.9
PVB composite	M1	833.3	79.4			182.5	119.0	363.5	11.9		0.4	0
	M2	833.3	79.4			182.5	119.0	363.5	11.9	4.2	0.4	0.3
	M3	833.3	79.4			182.5	119.0	363.5	11.9	8.3	0.4	0.6
	M4	833.3	79.4			182.5	119.0	363.5	11.9	12.5	0.4	0.9

Table 4
Physical and mechanical property of PVA fiber.

Fiber type	Diameter (mm)	Thickness (dtex)	Cut length (mm)	Tensile strength (N/mm^2)	Elongation (%)	Young's modulus (kN/mm^2)	Specific gravity
RECS15	0.04	15	8	1600	7	40	1.3

ment used is ASTM Type I normal Portland cement. The metakaolin (MK) conformed with the ASTM C-618 [32], Class N Specifications for Natural and Calcined Pozzolans. Sika ViscoCrete 2100 superplasticizer is used which meets the requirements for ASTM C-494 Types A and F [33]. The poly(vinyl butyral) (PVB) is Mowital B75H and Butvar B-79. Mowital is produced by Kuraray Specialities Europe (KSE). Butvar B-79 is provided by Solutia Inc. Table 3 lists some properties of PVB products. The poly(vinyl alcohol) (PVA) fibers used were manufactured by Kuraray Co. Ltd. of Japan. The type under this brand of the PVA fiber is RECS15, which has the properties listed in Table 4.

3.2. Experimental procedure

3.2.1. Compressive test

The compressive strengths are measured by testing 50 × 100 mm (2 by 4 in.) cylinders at a constant loading rate of 20 MPa/min (2900.7 psi/min). The test result is typically the average of at least three specimens. Young's modulus was not formally investigated but appeared to be significantly less than typical concretes.

3.2.2. Flexural test

The flexural stress is obtained from four-point bending test on 38 × 38 × 305 mm (1.5 × 1.5 × 12 in.) plain or PVB concrete beam at a loading rate of 445 N/min (100 lb/min), the corresponding stress increasing rate at the extreme fiber stress is 1.2 MPa/min (178 psi/min). Fig. 5 shows the experiment test set up for four-point bending. Specimens are loaded until fracture and load–deflection curves are recorded.

3.2.3. Fracture toughness test

According to ASTM E 399 [30], the fracture toughness test is performed on single edge V-notch bend (SENB) specimens. The configuration of the SENB specimen is shown in Fig. 6. The dimension of the specimens used in this research is 23 × 46 × 203 mm (0.9 × 1.8 × 8 in.) with a notch height to beam height (a/W) ratio equal to 0.5. The free span to beam height ratio is 4. The notched specimens are tested in three-point bending as shown in Fig. 7. Loading rate is 33 MPa m$^{0.5}$/min (30 ksi-in$^{0.5}$/min). Specimens are loaded until fracture load are recorded. Care is taken to produce a notch with a V shaped outline.

3.2.4. Charpy impact test

The Charpy U-notch test refers to the ASTM E23 [34], standard test methods for notched bar impact testing of metallic material and is used to determine fracture energy. The configurations of the specimen for the Charpy impact test are shown in Fig. 8. The loading configuration is shown is Fig. 9. Tinius Olsen "Change-O-Matic" impact testing machine (Fig. 10) is used in this test. After setting the specimen, the pendulum is released from a height y_1 and swings through the specimen to a height y_2. Assuming negligible friction and aerodynamic drag, the energy absorbed by the specimen is equal to the height difference times the weight of the pendulum.

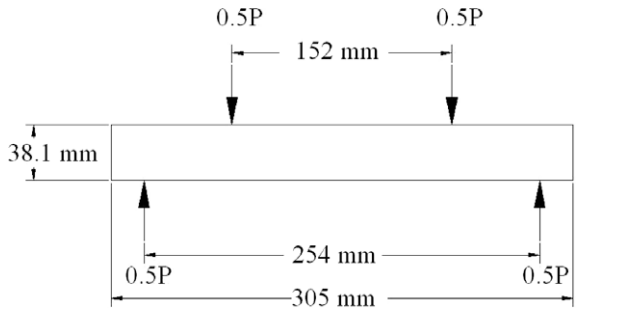

Fig. 5. Experiment set up for four-point bending.

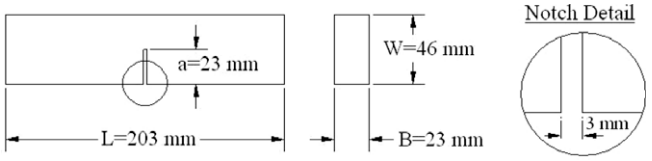

Fig. 6. Configurations of the single edge notch bend (SENB).

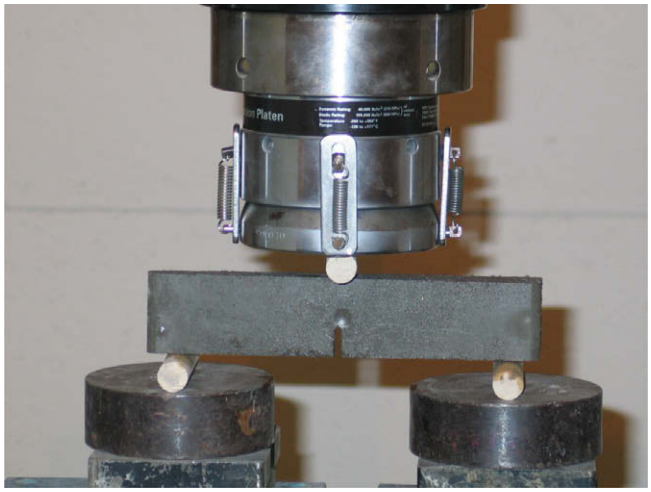

Fig. 7. Three points bending apparatus for testing single edge notch bend (SENB) specimens.

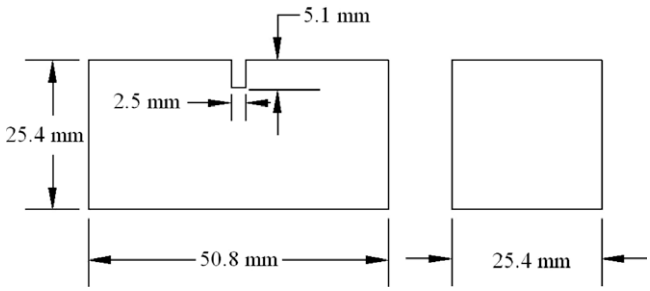

Fig. 8. Charpy U-notch specimen.

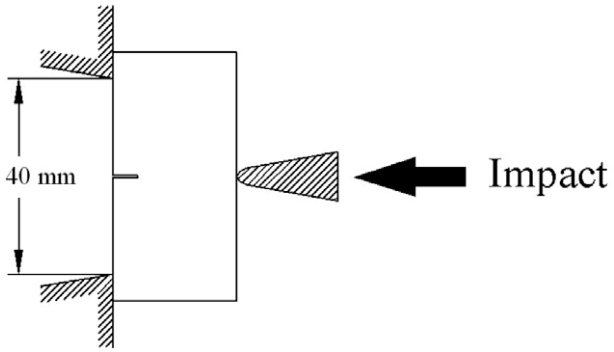

Fig. 9. Loading configuration for Charpy U-notch test.

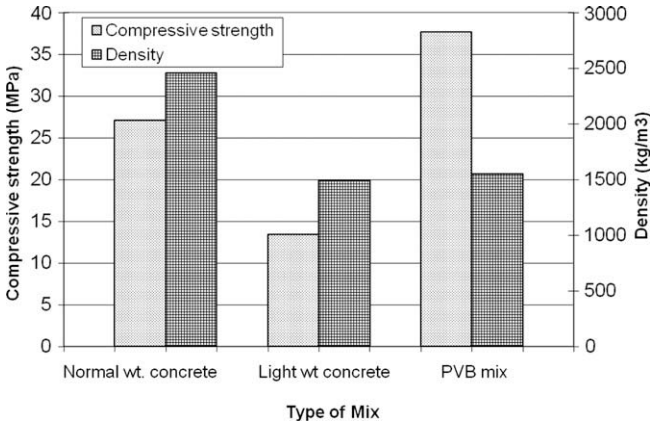

Fig. 11. The comparison of the compressive strength and density.

Fig. 10. Tinius Olsen "Change-O-Matic" impact testing machine.

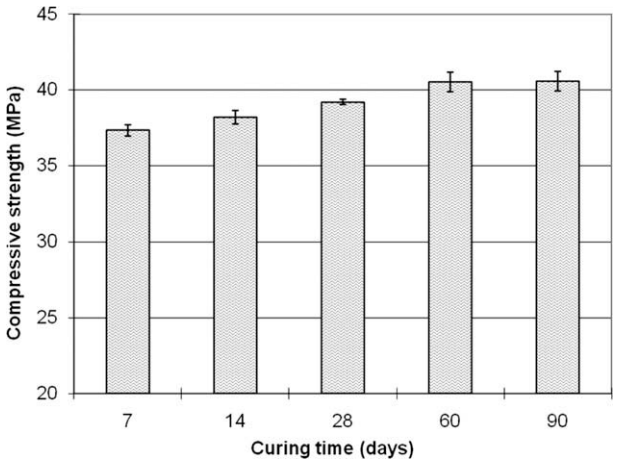

Fig. 12. Compressive strength with curing length.

4. Results and discussion

4.1. Compressive strength

As shown in Fig. 11, PVB composite, placed with no fiber (M1), has an average compressive strength of 37.7 MPa (5467.7 psi) with density about 1500 kg/m^3 (93.6 pcf) and water to cementitious ratio of 0.4. Compared with the lightweight concrete (L1) of 13.4 MPa with the same density and water to cementitious ratio, and the normal-weight concrete (N1) at 27.1 MPa (3930.4 psi) with density about 2500 kg/m^3 (156.1 pcf) and same water to cementitious ratio of 0.4, PVB composite shows better compressive strength. Fig. 12 shows the compressive strength of PVB composite (M1) with time. The results shows that compressive strength slightly increased with curing time, however, the increase in strength seems insignificant after 60 days.

4.2. Effect of PVA fibers on flexural load–deflection curves

The flexural load–deflection relationships determined with the four-point bending test are shown in Fig. 13. The addition of fiber to the PVB composite material caused an increase in the ultimate flexural load and deflection. The PVB composite shows higher improvement in both ultimate flexural load and deflection than lightweight concrete by the addition of PVA fiber. Toughness (ductility) is generally defined as energy adsorption capacity. It is calculated from the area under the load–deflection curve. The value is estimated by integrating the area under the load–deflection curve up to the point of collapse. Table 5 lists the result of flexural toughness. It can be seen that PVB composite has a higher flexural toughness compared with the lightweight concrete. The higher flexural toughness in the PVB composite is contributed by the higher bond at the interface between PVB aggregate and cement matrix, as well as the interface between PVA fiber, cement matrix and PVB aggregate which is not existed in the regular lightweight concrete. The improvement in flexural strength is attributed to the reinforcing effect created by the PVA fibers. Fig. 14 shows a photograph of the fracture surface in a specimen that contained fibers. Many of the fibers remained intact, indicating that they pulled away from the matrix, as opposed to rupturing along their length. Li and coworkers [35] demonstrated that oil coating of fibers can improve the ductility with lower interfacial bond values. Better ductility with higher interfacial bond value is obtained in this research, which implies that ductility is coming from a different mechanism not only the fiber slippage.

4.3. Effect of PVA fiber on fractural toughness

The fracture toughness of PVB composite is 0.389, 0.528, 0.691 and 0.800 MPa m$^{0.5}$ (0.354, 0.481, 0.629 and 0.728 ksi-in$^{0.5}$) with the fiber volume fraction in 0%, 0.3%, 0.6%, and 0.9%, respectively. The fracture toughness increased with the fiber volume fraction. The rate of improvement is 37%, 77% and108%, depending

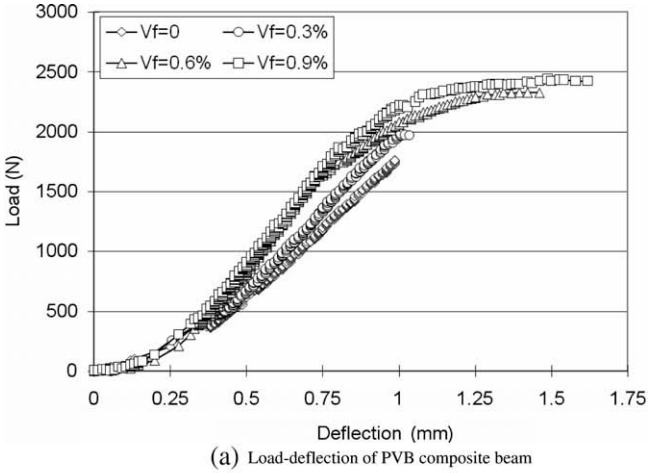

(a) Load-deflection of PVB composite beam

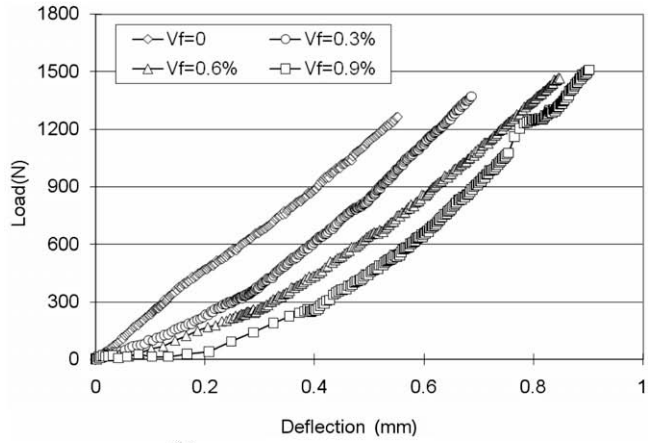

(b) Load-deflection of light weight concrete beam

Fig. 13. Flexural load–deflection curves.

Fig. 14. Fibers remain in tact along the fracture surface.

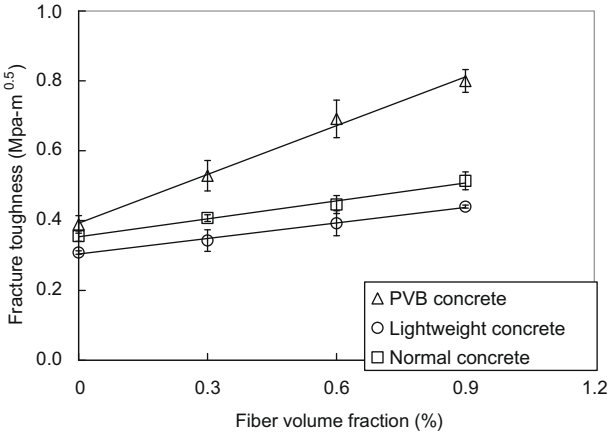

Fig. 15. Fracture toughness with fiber volume fraction.

Table 5
Flexural toughness.

	Flexural toughness (N mm)			
	V_f = 0%	V_f = 0.3%	V_f = 0.6%	V_f = 0.9%
PVB composite	993.3	1223.4	2321.6	2749.1
Lightweight concrete	436.4	548.3	726.2	995.3

on the fiber volume fraction. Compared with the fracture toughness of lightweight concrete and normal-weight concrete placed with no fiber, PVB composite has slightly higher fracture toughness. But the improvement of fracture toughness by the addition of PVA fiber is significant compared with the two groups at the same fiber volume fraction. It shows that in the PVB composite, there is a higher bond strength at the interface between fiber and the surrounding matrix. The increase in fracture toughness is found to be linear with increasing fiber volume fraction as shown in Fig. 15. Table 6 lists the results of the fracture toughness.

Table 6
Fracture toughness.

	Fracture toughness (MPa m$^{0.5}$)			
	V_f = 0%	V_f = 0.3%	V_f = 0.6%	V_f = 0.9%
PVB composite	0.389	0.528	0.691	0.800
Lightweight concrete	0.309	0.343	0.392	0.440
Normal-weight concrete	0.355	0.407	0.446	0.514

Table 7
Impact resistance.

	Impact energy (J)			
	V_f = 0%	V_f = 0.3%	V_f = 0.6%	V_f = 0.9%
PVB composite	14.9	17.6	21.0	31.9
Lightweight concrete	9.8	12.2	14.9	17.3
Normal-weight concrete	11.5	14.2	17.0	22.0

4.4. Effect of PVA fiber on impact resistance

The results in Table 7 shows that PVB composite have an average impact energy of 14.9 J (11.0 ft-lb), which is higher than the lightweight concrete of 9.8 J (7.3 ft-lb)and the normal-weight concrete of 11.5 J (8.5 ft-lb). The impact energy increases with the addition of the PVA fiber. Comparing with the lightweight concrete and normal-weight concrete, the improvement of impact energy is more significant in the PVB composite, which shows a non-linear increased with the addition of fiber (Fig. 16). The figure shows that the PVB composite matrix has a better impact resistance with addition of PVA fiber.

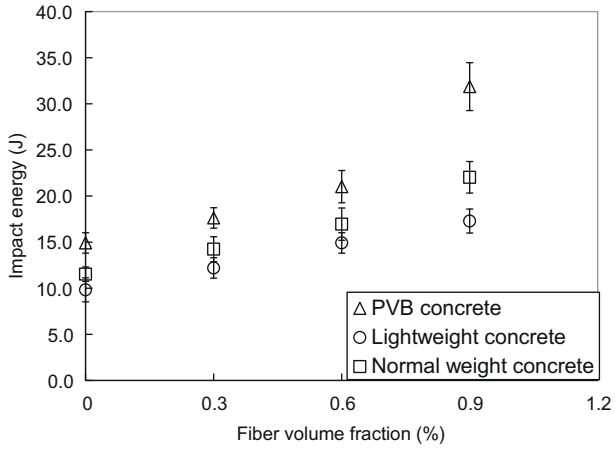

Fig. 16. The impact energy with the fiber volume fraction.

5. Fracture toughness model

The resistance to fracture of a material is known as its fracture toughness. It can be considered as a stress-based estimation derived from a function of the applied force and a specimen's geometry. Linear elastic fracture mechanics (LEFM) may be employed but this method is valid only as long as non-linear material deformation is confined to a small region surrounding the crack tip. There are other methods that can be used to estimate the fracture toughness, such as crack-tip-opening displacement (CTOD) and the J-integral formulation [31]. These methods are used to assess the elastic–plastic behavior of materials such as metals and alloys by considering crack-tip plasticity. But, because there is almost no plasticity developed in a brittle material such as concrete, a stress-based estimation of fracture toughness is developed herein. The formulation is based on a well-known concept called the "rule of mixtures" [29]. Although, many models have been developed based on this concept to calculate the tensile stress of fiber reinforced composites [36–38] little attention has been paid to models involving fracture toughness.

In prior work done on PVB/PVA materials, observations made in failed specimens revealed that many of the fibers remained intact; indicating that they pulled away from the matrix [1]. Thus, it can be construed that failure occurs as a result of fiber pull-out, where the fiber length used in the mix design is less than the critical fiber length.

Specifically, at the beginning of the loading process the matrix and fiber work together to resist the tensile stress. In this case, the stress is transferred from the matrix to the fiber via the fiber/matrix interface. But when loads are increased to the point at which the matrix begins to crack, the stress is transferred to the fibers alone. Since the fibers have a higher tensile strength than the friction bond strength at the interface, they pull-out of the matrix and failure occurs.

The tensile stress of the composite at mid-span in the single edge notched beam is given by Eq. (7), where the term ($\sigma_f V_f$,) represents the contribution made by the fibers. Assuming that pull-out dominates failure, this contribution may be described by Eq. (1). Making the appropriate substitution:

$$\sigma = \frac{1}{2} V_f g \tau \left(\frac{L_f}{d_f}\right) + \sigma_m (1 - V_f) \tag{10}$$

In Eq. (10), σ is the tensile stress of the composite which can be calculated according to beam theory as:

$$\sigma = \frac{M \cdot c}{I} \tag{11}$$

where c is the distance from the neutral axis to the extreme tensile fiber. Referring to the test and parameters described in conjunction with Eq. (8),

$$c = \frac{W - a}{2} \tag{12}$$

Consequently, Eq. (11) can be written as:

$$\sigma = \frac{M \cdot c}{I} = \frac{M \cdot \frac{W-a}{2}}{I} = \frac{PS(W-a)}{8I} \tag{13}$$

where P is the force at mid-span, S is the length of the free span, W is the height of the beam, and I is the centroidal moment of inertia parallel to the axis about which the moment is applied. The maximum tensile stress that the matrix can sustain is equal to:

$$\sigma_m = \frac{P_0 S(W-a)}{8I} \tag{14}$$

where P_0 is the failure load of a specimen placed without fiber.

Substituting Eqs. (13) and (14) into Eq. (10) yields:

$$\frac{PS(W-a)}{8I} = \frac{P_0 S(W-a)}{8I}(1 - V_f) + \frac{1}{2} V_f g \tau \left(\frac{L_f}{d_f}\right) \tag{15}$$

Thus, P can be expressed as,

$$P = \frac{8I}{(W-a)S}\left[\frac{P_0 S(W-a)}{8I}(1 - V_f) + \frac{1}{2} V_f g \tau \left(\frac{L_f}{d_f}\right)\right] \tag{16}$$

where the centroidal moment of inertia is calculated as follows:

$$I = \frac{1}{12} B (W-a)^3 \tag{17}$$

Substituting Eqs. (16) and (17) into Eq. (8) leads to the following expression for the fracture toughness:

$$K_{Ic} = \frac{2(W-a)^2}{3SW^{0.5}}\left[\frac{3P_0 S}{2B(W-a)^2}(1 - V_f) + \frac{1}{2} V_f g \tau \left(\frac{L_f}{d_f}\right)\right] f(a/W) \tag{18}$$

where $f(a/W)$ is the shape function expressed in Eq. (9).

6. Experimental vs. analytical results

In order to calculate the fracture toughness from Eq. (18), it is necessary to obtain the interfacial bond strength, τ which is defined as the friction between the fiber and the matrix. Although, the ultimate tensile strength is not measured directly herein, it can be estimated by the modulus of rupture R. Moreover, it is assumed that the tensile strength and the modulus of rupture of fiber reinforced concrete are very similar to those of plain concrete, since the volume fractions are relatively low (<2%) [39].

As discussed in the previous section, the tensile stress at the extreme fiber in the mid-span can be expressed as the summation of the tensile stress of the matrix and the fiber. Hence, the interfacial bond strength can be obtained from Eq. (10), provided that a flexural test is done to obtain the flexural stress. Table 8 shows the shear bond strength for the three materials tested, with and without fiber. It is evident that the PVB mix has a higher interfacial bond strength than that of lightweight and normal concrete. Table 9 shows the results of the fracture toughness data calculated from Eq. (18) expressed as a function of the fiber volume fraction. Table 10 lists the theoretical results obtained from these expressions along with the average values obtained from the tests. Table 11 lists the fracture toughness data from other references. Fracture toughness of basalt, glass and steel fiber with different fiber aspect ratio and matrix material are applied and calculated. The results show a good correlation with the test data. Fig. 17 includes data taken from all specimens (3) of each type and data from other

Table 8
Interfacial bond strength.

	Flexural stress σ (MPa)				g^*	L_f/d_f	τ (MPa)
	V_f = 0%	V_f = 0.3%	V_f = 0.6%	V_f = 0.9%			
PVB composite	4.07	5.36	6.63	7.56	1.5	200	2.79
Lightweight concrete	2.35	3.02	3.70	4.03	1.5	200	1.42
Normal-weight concrete	2.06	3.02	3.58	4.44	1.5	200	1.86

* According to Kanda and Li [40].

Table 9
Theoretical fracture toughness.

	P_0 (N)	g^*	L_f/d_f	τ (MPa)	K_{Ic} (MPa m$^{0.5}$)
PVB composite	178.4	1.5	200	2.79	$0.39 + 39.3V_f$
Lightweight concrete	141.6	1.5	200	1.42	$0.31 + 19.9V_f$
Normal-weight concrete	163.1	1.5	200	1.86	$0.36 + 26.1V_f$

* According to Kanda and Li [40].

Table 10
Comparison of fracture toughness.

	Source	Fracture toughness (MPa m$^{0.5}$)			
		V_f = 0%	V_f = 0.3%	V_f = 0.6%	V_f = 0.9%
PVB concrete	Calculation	0.389	0.507	0.625	0.743
	Test	0.389	0.528	0.691	0.800
Lightweight concrete	Calculation	0.308	0.368	0.428	0.487
	Test	0.309	0.343	0.392	0.440
Normal-weight concrete	Calculation	0.356	0.434	0.513	0.591
	Test	0.356	0.407	0.446	0.514

references, clearly illustrating that the results from the model compare well with the test data.

7. Conclusion

Poly(vinyl butyral) (PVB) and PVA fibers are used as fine aggregate and reinforcement to develop a novel cementitious material in this study to test whether organic non-siliceous aggregates with different chemical properties than typical sands will influence mechanical properties of concrete. Mechanical properties are tested and a fracture model is developed. The fracture toughness of PVB cementitious composites compares favorably with literature values for other types of composites with differing fiber and matrix types, made from a geopolymer with basalt fiber (Dias), a polyester polymer with glass (Griffiths) and concrete with steel (Taylor). The PVB material with fibers produced the greatest change in fracture toughness from baseline at the lowest fiber volume fraction. Taken together these results suggest that the interaction between matrix and fiber differs in this composite compared

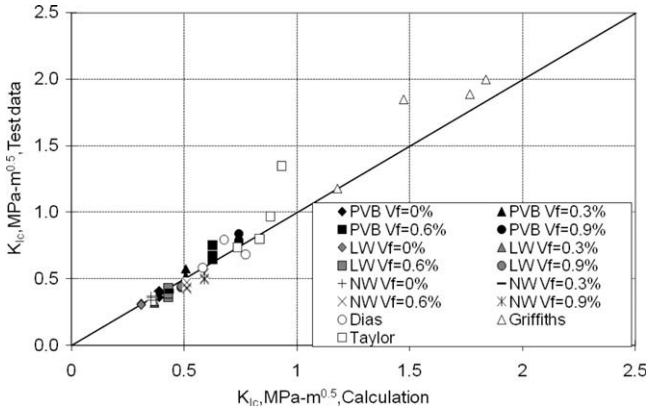

Fig. 17. Comparison of fracture toughness.

to the other composites and that the PVB/fiber interaction is highly efficient.

Lightweight concrete with the same density as PVB concrete and normal-weight concrete are produced and tested to make comparisons with PVB composite concrete. Because all of the samples have the same fiber (when present) and cement paste, in this way fiber matrix interactions are held constant and only fiber aggregate and aggregate to paste interactions are investigated. When we compare the results for lightweight and PVB aggregates, we find that several mechanical properties suggest much different interactions between paste and aggregate and aggregate and fiber for the two types of aggregate. On examination of Fig. 13a and b, we observe that at zero volume fraction, the deflection at fracture with PVB alone is about double the deflection for the same beam made with a lightweight aggregate. Similarly we observe that fracture toughness and impact energy are all higher at zero volume fraction fiber with the PVB aggregate versus the lightweight aggregate. With increasing fiber volume fraction, the differences between the aggregates are magnified. As shown in Fig. 13a and b, during deflection at 0.9% fiber, lightweight aggregate concrete suddenly fails, but concrete beams made with PVB and PVA fibers continue deflecting with constant load. This pattern of constant load with deflection is not seen with the lightweight mortar. The area under the

Table 11
Fracture toughness data from other references.

	Fiber type	Matrix type	L_f/d_f	τ (MPa)	Fracture toughness (MPa m$^{0.5}$)							
					Cal.	Test	Cal.	Test	Cal.	Test	Cal.	Test
Dias and Thaumaturgo [41]	Basalt	Polymeric concrete	500	0.27	V_f = 0%		V_f = 0.5%		V_f = 1%			
					0.582	0.582	0.678	0.794	0.773	0.684		
Griffiths and Ball [42]	Glass	Polyester concrete	400	1.21	V_f = 0%		V_f = 2%		V_f = 2%		V_f = 2%	
					1.18	1.18	1.474	1.850	1.838	2.000	1.767	1.890
Taylor et al. [43]	Steel	High strength concrete	60	3.09	V_f = 0%		V_f = 0.5%		V_f = 0.8%		V_f = 1%	
					0.737	0.737	0.834	0.800	0.883	0.968	0.932	1.347

curve which represents stored energy is at least doubled during deflection of the PVB/fiber composite when compared to the lightweight aggregate and also doubled relative to PVB concrete without fiber. These observations suggest that interactions between the PVB and paste matrix and PVB and fiber allow a mechanism to store this energy, which is likely due to the creation of non-covalent bonds between these substrates. Similar results are seen in the fracture toughness studies and the impact studies. In Fig. 15, as fiber is added to the PVB composite, the slope for the changes in fracture toughness is greater than the slopes for the regular and lightweight aggregate concretes, meaning that more internal chemical interactions are generated in the PVB composite than the other two concretes. Impact energy, Fig. 16, shows the same effect. Taken together, these observations support the concept that significantly different chemical interactions between paste and aggregate and fiber and aggregate are seen in the PVB/PVA fiber composite than are seen in regular concrete. Although direct observations of the ITZ have not been performed, it is reasonable to conclude that the improved mechanical effects with PVB/PVA fiber concrete have to have their basis in improved bonding between paste and aggregate and fiber and aggregate. Since it is the interfacial transition zone which regulates chemical bonding between paste and aggregate and fiber and paste, we would speculate that the mechanical differences we see can be attributed to improved ITZ bonding.

Several conclusions can be outlined according to this study:

1. PVB cementitious composite, placed with no fiber, has higher compressive strength, flexural strength, fracture toughness and impact resistance but lower density than the lightweight concrete and normal-weight concrete of the same water to cementitious ratio. This implies that PVB, when used as an aggregate, bonds very well with the cement matrix. This is attributed to the fact that PVB contains hydroxyl groups which have the potential to form hydrogen bonds between molecules. Additional effects on the cement matrix itself may occur through available ether group interactions which may alter the cement matrix structure or nucleation reaction.
2. Compared with the lightweight concrete and normal-weight concrete, the addition of PVA fiber has a higher improvement on the flexural strength, fracture toughness and impact resistance. With the addition of the same volume fraction of PVA, the flexural strength, fracture toughness and impact resistance of PVB is better than those properties associated with lightweight and normal concretes. This implies that the PVB composite has a higher bond at the fiber/matrix interface.
3. The increase in fracture toughness is found to be linear with increasing fiber volume fraction whereas the increase associated with the impact resistance is non-linear. Significant improvements in both of these parameters indicate that chopped fibers can play important roles in resisting dynamic loads.
4. The fracture toughness model developed in this study showed a good correlation with the fracture toughness tests and the data from other references. However, more experimental data must be collected to further verify the model.
5. PVB/PVA fiber cementitious composites have almost twice the fracture toughness of regular fibered cement mortars despite having almost half the density.

However, PVB is an experimental substance used to illuminate effects within cement pastes. Because of its expense, it cannot be recommended as a civil engineering material but it may have specialized uses.

References

[1] Lavin T, Toutanji H, Xu B, Ooi T, Biszick K, Gilbert J. Matrix design for strategically tuned absolutely resilient structures (STARS). In: Proceedings: SEM XI international congress and exposition on experimental and applied mechanics, Paper No. 71, Orlando, FL, 2–5 June 2008.

[2] Toutanji H, Xu B, Gilbert J, Lavin T. Fracture toughness model for poly(vinyl alcohol) fiber reinforced high-performance cementitious material. In: Proceedings: 8th international symposium on utilization of high-strength and high-performance concrete, Paper No.133, Tokyo, Japan, 27–29 October 2008.

[3] Breton D, Carles-Gibergues A, Ballivy G, Grandet J. Contribution to the formation mechanism of the transition zone between rock and cement paste. Cem Concr Res 1993;23:335–46.

[4] Richard JS. Purifying proteins for proteomics: a laboratory manual. Cold spring harbor, New York: CSHL Press; 2004. p. 73.

[5] Sun Z, Garboczi EJ, Shah SP. Modeling the elastic properties of concrete composites: experiment, differential effective medium theory, and numerical simulation. Cem Concr Compos 2007;29(1):22–38.

[6] Leemann A, Münch B, Gasser P, Holzer L. Influence of compaction on the interfacial transition zone and the permeability of concrete. Cem Concr Res 2006;36(8):1425–33.

[7] Elsharief A, Cohen MD, Olek J. Influence of aggregate size, water cement ratio and age on the microstructure of the interfacial transition zone. Cem Concr Res 2003;33(11):1837–49.

[8] Nadeau JC. Water–cement ratio gradients in mortars and corresponding effective elastic properties. Cem Concr Res 2002;32(3):481–90.

[9] Bela F, Arliguie G, François R. Porous structure of the ITZ around galvanized and ordinary steel reinforcements. Cem Concr Res 2001;31(11):1561–6.

[10] Diamond S, Huang JD. The ITZ in concrete – a different view based on image analysis and SEM observations. Cem Concr Compos 2001;23(2–3):179–88.

[11] Harutyunyan VS, Abovyan ES, Monteiro PJM, Mkrtchyan VP, Balyan MK. Microstrain distribution in calcium hydroxide present in the interfacial transition zone. Cem Concr Res 2000;30(5):709–13.

[12] Scrivener KL, Nemati KM. The percolation of pore space in the cement paste/aggregate interfacial zone of concrete. Cem Concr Res 1996;26(1):35–40.

[13] Akçaolu T, Tokyay M, Çelik T. Effect of coarse aggregate size on interfacial cracking under uniaxial compression. Mater Lett 2002;57(4):828–33.

[14] Akçaolu T, Tokyay M, Çelik T. Effect of coarse aggregate size and matrix quality on ITZ and failure behavior of concrete under uniaxial compression. Cem Concr Res 2004;26(6):633–8.

[15] Tasong WA, Lynsdale CJ, Cripps JC. Aggregate–cement paste interface: part I. Influence of aggregate geochemistry. Cem Concr Res 1999;29:1019–25.

[16] Bentz DP. Influence of silica fume on diffusivity in cement-based materials. II. Multi-scale modeling of concrete diffusivity. Cem Concr Res 2000;30(7):1121–9.

[17] Asbridge AH, Chadbourn GA, Page CL. Effects of metakaolin and the interfacial transition zone on the diffusion of chloride ions through cement mortars. Cem Concr Res 2001;31(11):1567–72.

[18] Poon C, Lam L, Kou SC, Wong Y, Wong R. Rate of pozzolanic reaction of metakaolin in high-performance cement paste. Cem Concr Res 2001;31:1301–6.

[19] Friedrich K, Fakirov S, Zhang Z. Polymer composites: from nano-to-macro-scale. New York: Springer Inc.; 2005.

[20] Mark JE. Polymer data handbook. Oxford University Press, Inc.; 1999.

[21] Cho CW, Cho YS, Yeo JG, Kimb J, Paik U. Effects of PVB on the gelation behavior of $BaTiO_3$-based dielectric particles and glass suspension. J Eur Ceram Soc 2003;23(13):2315–22.

[22] Cho Chae-Woong, Cho Yong-Sang, Yeo Jeong-Gu, Choi Sung-Churl, Kim Jonghee, Paik Ungyu. The role of 2-methyl-2,4-pentanediol modifier and its interaction with poly(vinyl butyral) binder in $BaTiO_3$ and $Li_2O–B_2O_3–BaO–SiO_2$ glass suspensions. Colloid Surf A: Physicochem Eng Aspects 2003;224(1–3):83–91.

[23] Zheng ZH, Feldman D. Synthetic fiber-reinforced concrete. Prog Polym Sci 1995;20:185–210.

[24] Feldman D, Barbalata A. Synthetic polymers: technology, properties, applications. London: Chapman and Hall; 1996. 101.

[25] Wang SX, Li VC. Polyvinyl alcohol fiber reinforced engineered cementitious composites: material design and performances. In: Fischer G, Li VC, editors, Proceedings: international RILEM workshop on high performance fiber reinforced cementitious composites in structural applications. RILEM Publications SARL; 2006. p. 65–73.

[26] Li VC. Large volume high performance applications of fibers in civil engineering. J Appl Polym Sci 2002;83:660–86.

[27] Lin Z, Li VC. Crack bridging in fiber reinforced cementitious composites with slip-hardening interface. J Mech Phys Solids 1997;45(5):763–87.

[28] De Koker D, Van Zijl GPAG. Extrusion of engineered cement-based composite material. In: 6th RILEM symposium on fiber-reinforced concretes (FRC), Varenna, Italy. September 20–22, 2004. p. 1301–10.

[29] Sun Z, Garboczi EJ, Shah SP. Modeling the elastic properties of concrete composites: experiment, differential effective medium theory, and numerical simulation. Cem Concr Compos 2007;29(1):22–38.

[30] ASTM E399. Standard test method for linear-elastic plane-strain fracture toughness K1c of metallic materials. American society for testing and materials standards annual books, vol. 03.01.
[31] Anderson TL. Fracture mechanics. Taylor and Francis Group; 2005. p. 288–9.
[32] ASTM C618. Standard specification for coal fly ash and raw or calcined natural pozzolan for use in concrete. American society for testing and materials standards annual books, vol. 04.02.
[33] ASTM C494. Standard specification for chemical admixtures for concrete. American society for testing and materials standards annual books, vol. 04.02.
[34] ASTM E23. Standard test methods for notched bar impact testing of metallic materials.
[35] Redon C, Li VC, Wu C, Hoshiro H, Saito T, Ogawa A. Measuring and modifying interface properties of PVA fibers in ECC matrix. J Mater Civ Eng (ASCE) 2001;November/December:399–406.
[36] Facca AG, Kortschot MT, Yan N. Predicting the tensile strength of natural fiber reinforced thermoplastics. Compos Sci Technol 2007;67(11–12):2454–66.
[37] Madsen B, Hoffmeyer P, Lilholt H. Hemp yarn reinforced composites-ii. Tensile properties. Compos Part A: Appl Sci Manuf 2007;38(10):2204–15.
[38] Mouhmid B, Imad A, Benseddiq N, Benmedakhène S, Maazouz A. A study of the mechanical behavior of a glass fiber reinforced polyamide 6,6: experimental investigation. Polym Test 2006;25(4):544–52.
[39] Arisoy B, Wu HC. Material characteristics of high performance lightweight concrete reinforced with PVA. Constr Build Mater 2008;22(4):635–45.
[40] Kanda T, Li VC. Practical design criteria for saturated pseudo strain hardening behavior in ECC. J Adv Concr Technol 2006;4(1):59–72.
[41] Dias DP, Thaumaturgo C. Fracture toughness of geopolymeric concretes reinforced with basalt fibers. Cem Concr Compos 2005;27:49–54.
[42] Griffiths R, Ball A. An assessment of the properties and degradation behaviour of glass-fiber-reinforced polyester polymer concrete. Compos Sci Technol 2000;60:2747–53.
[43] Taylor M, Lydon FD, Barr BIG. Toughness measurements on steel fibre-reinforced high strength concrete. Cem Concr Compos 1997;19:329–40.